Using Block Copolymer Micellar Thin Films as Templates for the Production of Catalysts for Carbon Nanotube Growth

R. D. Bennett,† G. Y. Xiong,‡ Z. F. Ren,‡ and R. E. Cohen*,†

Department of Chemical Engineering, Massachusetts Institute of Technology, Cambridge, Massachusetts 02140, and Department of Physics, Boston College, Chestnut Hill, Massachusetts 02467

Received June 24, 2004. Revised Manuscript Received October 4, 2004

We report a novel approach that uses block copolymer micelles as a means to create large area arrays of iron-containing nanoclusters capable of catalyzing the growth of carbon nanotubes (CNTs). The amphiphilic block copolymer poly(styrene-*block*-acrylic acid) (PS-*b*-PAA) forms micelles in solution which are capable of self-organizing into ordered structures on surfaces. By spin-coating these solutions onto a variety of substrates, we can create quasi-hexagonal arrays of PAA spheres within a PS matrix. The carboxylic acids groups in the PAA domains can be utilized in an ion-exchange protocol to selectively sequester iron ions, which results in iron-containing nanoclusters that are nearly monodisperse in size (diameter ∼8 nm) and patterned at a density of approximately 10^{11} particles per cm^2. In principle, this route for synthesizing iron-containing nanoclusters offers the capability of controlling the cluster size and spacing by altering the molecular weight of the block copolymer. In this report, we demonstrate the ability of these block-copolymer-templated iron-containing nanocluster arrays to catalyze the growth of CNTs in a thermal chemical vapor deposition (CVD) process. We present transmission electron microscope (TEM) and scanning electron microscope (SEM) images of the as-grown CNTs still attached to their growth substrate, which allows us to characterize both the CNTs and the catalytic nanoclusters after CVD growth.

Introduction

Carbon nanotubes (CNTs) have been the focus of intense research since their discovery in 1991,[1] and many potential applications, such as field emission,[2] hydrogen storage,[3] and microelectronics,[4] seek to exploit the unusual set of mechanical, structural, and electronic properties that CNTs possess. Although there are multiple methods for synthesizing CNTs, chemical vapor deposition (CVD) is the most widely used because of its ease of operation and its scale-up capability. In CVD, metal nanoparticles (namely iron, cobalt, and nickel) are required to catalyze the growth of CNTs, so the ability to control the size and patterning of surface-bound metal nanoparticles is an essential task.

One of the most common routes for creating the surface arrays of metal nanoparticles involves, as a first step, depositing a thin layer of metal on a surface using magnetron sputtering.[5−7] Upon heating, the metal film forms metal nanoparticles, which are then capable of catalyzing the growth of CNTs. Although this method is straightforward, it offers little control over the size or spacing of the metal nanoparticles, and patterned nanoparticle arrays are not achievable.

Alternative procedures for creating metal nanoparticles have been developed recently in an attempt to gain better control over the size and spacing of the metal nanoparticles. Ren and co-workers[8] have used polystyrene nanosphere masks to deposit large periodic arrays of nickel nanoparticles with diameters between 50 and 100 nm. Ren and co-workers[9] have also used electrochemical deposition to create Ni nanoparticles with controlled site density between about 10^6 and 10^8 nanoparticles per cm^2, although the nanoparticles are randomly located and have diameters ranging from less than 50 nm to up to 200 nm. Lieber and co-workers[10] created nearly monodisperse diameter iron nanoclusters with diameters between 3 and 13 nm in organic solvents by thermal decomposition of iron pentacarbonyl, and

* To whom correspondence should be addressed: recohen@mit.edu.
† Massachusetts Institute of Technology.
‡ Boston College.

(1) Iijima, S. *Nature* **1991**, *354*, 56−58.
(2) DeHeer, W. A.; Chatelain, A.; Ugarte, D. *Science* **1995**, *270*, 1179−1180.
(3) Dillon, A. C.; Jones, K. M.; Bekkedahl, T. A.; Kiang, C. H.; Bethune, D. S.; Heben, M. J. *Nature* **1997**, *386*, 377−379.
(4) Tans, S. J.; Verschueren, A. R. M.; Dekker, C. *Nature* **1998**, *393*, 49−52.
(5) Ren, Z. F.; Huang, Z. P.; Xu, J. W.; Wang, J. H.; Bush, P.; Siegal, M. P.; Provencio, P. N. *Science* **1998**, *282*, 1105−1107.
(6) Huang, Z. P.; Wang, D. Z.; Wen, J. G.; Sennett, M.; Gibson, H.; Ren, Z. F. *Appl. Phys. A* **2002**, *74*, 387−391.
(7) Hofmann, S.; Ducati, C.; Robertson, J.; Kleinsorge, B. *App. Phys. Lett.* **2003**, *83*, 135−137.
(8) Huang, Z. P.; Carnahan, D. L.; Rybczynski, J.; Giersig, M.; Sennett, M.; Wang, D. Z.; Wen, J. G.; Kempa, K.; Ren, Z. F. *App. Phys. Lett.* **2003**, *82*, 460−462.
(9) Tu, Y.; Huang, Z. P.; Wang, D. Z.; Wen, J. G.; Ren, Z. F. *Appl. Phys. Lett.* **2002**, *80*, 4018−4020.
(10) Cheung, C. L.; Kurtz, A.; Park, H.; Lieber, C. M. *J. Phys. Chem. B* **2002**, *106*, 2429−2433.

10.1021/cm048992l CCC: $27.50
Published on Web 11/25/2004

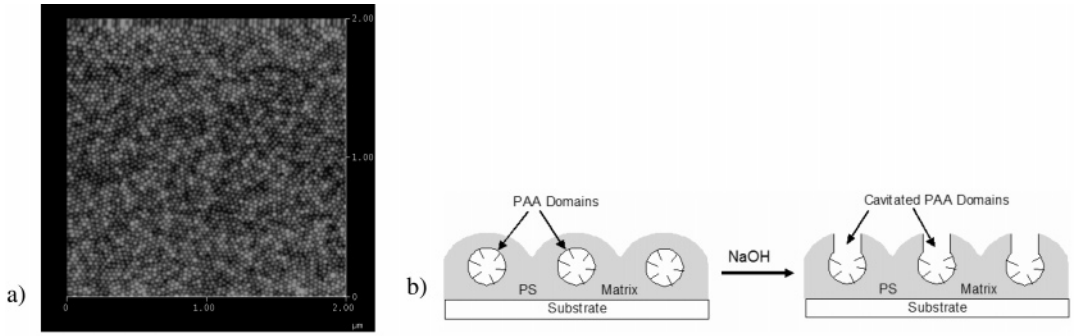

Figure 1. (a) AFM image of noncavitated thin film on silicon nitride substrate (scan size of 2 μm by 2 μm). (b) Diagram illustrating the cavitation step caused by submerging the thin films in $NaOH_{(aq)}$ solution.

then deposited the nanoparticles onto a silicon substrate. In another approach, Dai and co-workers[11] created iron oxide nanoparticles with diameters of 1−2 nm by soaking silicon oxide substrates in a solution of hydroxylamine and $FeCl_3$. Dai and co-workers[12] have also used the iron-storage protein, ferritin, to create discrete iron oxide nanoparticles which are catalytically active toward single wall CNT growth. Hinderling et al.[13] used a specially synthesized polystyrene-*block*-polyferrocenyldimethylesilane diblock copolymer to produce 30-nm iron oxide nanoparticles on silicon substrates that could be subsequently used to catalyze carbon nanotube growth.

Here we report a simple approach that uses block copolymer micelles as a template to create large area arrays of metal nanoclusters capable of catalyzing the growth of multiwall CNTs. Our route for producing metal nanocluster arrays relies on the ability of amphiphilic block copolymers, such as poly(styrene-*block*-acrylic acid) (PS-*b*-PAA), to form micelles in solution which are capable of self-organizing into partially ordered structures on surfaces.[14] Owing to the slow exchange kinetics in block copolymer micelles, we are able to transfer the micelles from colloidal solution onto a substrate using a spin-casting process. This allows for the creation of quasi-hexagonal arrays of PAA spheres within a PS matrix. As shown previously,[14,15] by submerging the polymer thin films in an aqueous metal salt solution, the carboxylic acids groups in the PAA domains can be utilized in an ion-exchange protocol to selectively sequester a variety of metal cations. The polymer can then be removed using thermal degradation or oxygen plasma etching, resulting in arrays of metal-containing nanoclusters that are nearly monodisperse in size and patterned at a density of approximately 10^{11} particles per cm^2. In principle, this route for synthesizing metal nanoclusters offers the capability of tuning the size and spacing between the metal nanoclusters by altering the molecular weight of the block copolymer,[16] which would lead to control over the size and spacing of the CNTs formed. Appropriate masking or stamping transfer techniques allow for the straightforward production of patterned arrays of the micellar block copolymer templates and, therefore, of the CNTs produced subsequently.

In this report, we examine the effectiveness of block-copolymer-templated metal nanocluster arrays in catalyzing the growth of multiwall CNTs in a thermal CVD process. We present scanning electron microscope (SEM) and transmission electron microscope (TEM) images of the as-grown CNTs still attached to their growth substrate, as well as high-resolution TEM images of the multiwall CNTs.

Experimental Section

Materials. Poly(styrene-*block*-acrylic acid) (PS-*b*-PAA) (M_n(PS) = 16 400 g/mol, M_n(PAA) = 4500 g/mol, PDI = 1.05) was used as received from Polymer Source, Inc. The following chemicals were also used as received: anhydrous iron(III) chloride obtained from Sigma-Aldrich Co., lead(II) acetate trihydrate obtained from Sigma-Aldrich Co., sodium hydroxide (98.9%) obtained from Mallinckrodt, and toluene (HPLC grade, 99.8%) obtained from Sigma-Aldrich Co. The silicon nitride membrane window substrates were purchased from Structure Probe, Inc. Each substrate (surface area ~4.5 mm^2) consisted of a 100-nm-thick amorphous, low-stress Si_3N_4 membrane supported on a 0.2-mm-thick silicon wafer that had been back-etched in the center to create the electron transparent Si_3N_4 window (surface area ~0.2 mm^2). The use of the electron-transparent silicon nitride substrates allows for direct TEM characterization without disturbing the spin-cast films. Polished silicon wafers of ⟨100⟩ orientation from Nestec, Inc. were also used as received. Each substrate was rinsed with toluene prior to film casting. All aqueous solutions were made using deionized water (>18 MΩ cm, Millipore Milli-Q). Lacey carbon films were used as received from Electron Microscopy Sciences.

Sample Preparation. The sample preparation followed a procedure developed previously,[14] with adjustments (discussed below) to improve substrate wetting, and, consequently, the surface coverage of the metal nanoclusters. The block copolymer was mixed with toluene at a concentration of 12.5−15 mg/mL, resulting in a slightly cloudy solution. By heating the solution to ~145 °C for 20 min, the solution became clear, and it remained clear after cooling to room temperature. Previous work[14] demonstrated that this transition in solution optical properties corresponds to a change from cylindrical to spherical block copolymer micelles. Thin films were then created by spin-casting the micellar solution onto the substrates. The resulting morphology can be seen in Figure 1a. The film thicknesses were approximately 20 nm, as determined by atomic force microscope (AFM). Residual toluene was then removed under vacuum.

Two different methods were used to load the metal species into the polymer thin films. In the first, the polymer thin films

(11) Choi, H. C.; Kundaria, S.; Wang, D. W.; Javey, A.; Wang, Q.; Rolandi, M.; Dai, H. J. *Nano Lett.* **2003**, *3*, 157−161.
(12) Li, Y. M.; Kim, W.; Zhang, Y. G.; Rolandi, M.; Wang, D. W.; Dai, H. J. *J. Phys. Chem. B* **2001**, *105*, 11424−11431.
(13) Hinderling, C.; Keles, Y.; Stockli, T.; Knapp, H. F.; de los Arcos, T.; Oelhafen, P.; Korczagin, I.; Hempenius, M. A.; Vancso, G. J.; Pugin, R.; Heinzelmann, H. *Adv. Mater.* **2004**, *16*, 876−879.
(14) Boontongkong, Y.; Cohen, R. E. *Macromolecules* **2002**, *35*, 3647−3652.
(15) Clay, R. T.; Cohen, R. E. *Supramol. Sci.* **1998**, *5*, 41−48.
(16) Khougaz, K.; Zhong, X. F.; Eisenberg, A. *Macromolecules* **1996**, *29*, 3937−3949.

were submerged in a 0.007 M $NaOH_{(aq)}$ solution for 16 h (subsequently referred to as a "cavitated" template). When the thin film is exposed to the $NaOH_{(aq)}$ solution, the PAA domains swell,[17] and because this cannot be accommodated by the glassy PS matrix, the swelling leads to the rupture of the PAA domains to the surface. This cavitation step is illustrated in Figure 1b, and was discussed in detail previously by Boontongkong et al.[14] These cavitated polymer thin films were then rinsed in deionized water for 1 min, submerged in a 0.5 mM $FeCl_3$ solution for 5 min, and then rinsed in deionized water for 2 min. The second route bypassed the cavitation step; the spin-coated films (subsequently referred to as a "noncavitated" template) were submerged directly into 0.5 mM $FeCl_3$ for 60 min, and then rinsed for 2 min in deionized water. For the cavitated thin films, the Fe^{3+} ions in solution exchange directly with the Na^+ ions of the carboxylic acid groups, while in the noncavitated thin films the Fe^{3+} ions diffuse through a thin PS layer before exchanging with the H^+ ions from the carboxylic acid groups. After the metal loading steps, the substrates were heated in air at 550 °C for 20 min to degrade the polymer and to convert the iron ions into iron oxide nanoclusters. The resulting nanocluster arrays were then characterized using TEM and AFM. A control substrate was also created by following the sample preparation steps listed above while omitting the iron ion loading step.

The nanocluster arrays were then used as catalytic substrates for the synthesis of CNTs using thermal CVD in a quartz-tube reactor. The chamber was pumped down to 0.1 Torr before raising the temperature to 750 °C. Once the reactor reached 750 °C, NH_3 gas was delivered to the reactor at 80 sccm for 10 min, and then C_2H_2 (feed gas) was added at 20 sccm for the duration of the growth. Growth times of 10, 30, and 60 min were used. After the growth, the samples were allowed to cool to 250 °C under vacuum and then removed from the reactor. Specimens for high-resolution TEM were prepared by sonicating the substrates containing CNTs in 2-propanol for 20 min, and then solvent-casting the CNTs onto lacey carbon films.

Microscopy. TEM was performed on a JEOL 200CX operating at 200 kV, a JEOL 2000FX operating at 200 kV, and a JEOL 2010 operating at 200 kV. SEM was performed on a JEOL 6320 FEG-SEM operating at 5 kV. AFM was performed on a Digital Instruments Dimension 3000 Nanoscope IIIA scanning probe microscope operating in tapping mode using a silicon cantilever (nominal tip radius of 5−10 nm).

Results

Catalytic Substrates. The AFM image of Figure 1a shows the nanoscale surface topology that results when the PS-*b*-PAA solution is spin-coated onto a silicon nitride substrate. This image shows the presence of spherical objects with an average diameter of 18 nm. As illustrated in Figure 1b, the PAA domains are expected[14] to have a somewhat smaller diameter than the AFM image suggests. This was confirmed by staining the PAA domains using a $PbAc_2$ solution, as shown in the TEM image in Figure 2. The stained PAA domains have diameters of approximately 12−14 nm. Figure 2 also demonstrates the quasi-hexagonal array of the PAA domains within the PS matrix. This spatial arrangement is maintained over >95% of the substrate surface.

In this report, nanocluster arrays for CNT growth were produced using both cavitated and noncavitated thin films as templates. In both of these synthesis routes, similar iron oxide nanocluster arrays were produced. Figure 3a shows a TEM image of an iron-containing nanocluster array produced by loading a cavitated thin film with iron and then thermally degrading the polymer in air at 550 °C for 20 min. The heating step removes the polymer and leaves behind iron-containing nanoclusters with diameters of 7.5 ± 0.8 nm and center-to-center spacings of 30−35 nm. The areal density is approximately 10^{11} nanoclusters per cm^2 and the nanocluster patterning is retained over nearly the entire substrate during the heating step. For the iron oxide nanocluster arrays synthesized from noncavitated arrays, it should be noted that approximately 75−80% of the substrate surface shows nanoclusters arranged in the quasi-hexagonal array similar to Figure 3a, while 20−25% of the substrate has nanoclusters which are completely disordered, as shown in Figure 3b. For reasons not yet understood, this loss of ordering on the substrate surface is seen only in the nanocluster arrays produced using the 550 °C heat treatment on noncavitated thin films, and not in the nanocluster arrays created using cavitated thin films.

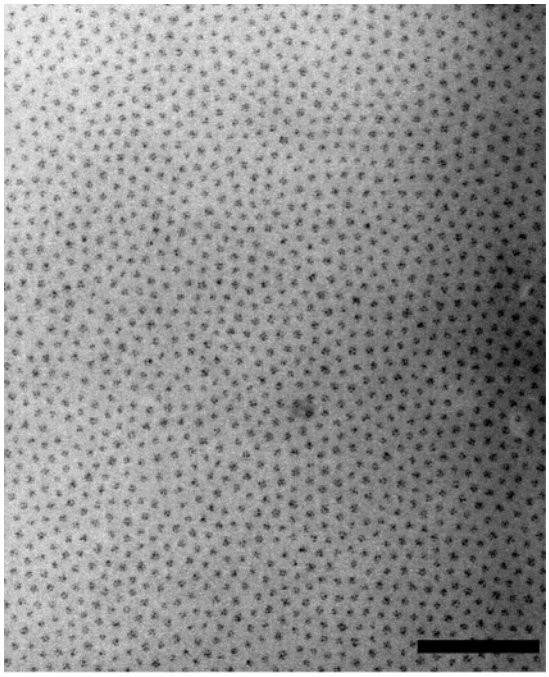

Figure 2. TEM image of Pb nanocluster array created from a noncavitated thin film, scale bar = 200 nm. Lead was used in place of iron because it offers enhanced contrast in the TEM. In addition, it demonstrates the general receptivity of the PS-*b*-PAA block copolymer to a variety of metal cations (refs 14 and 15).

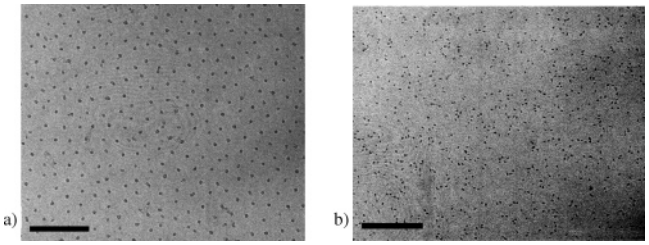

Figure 3. TEM images of iron oxide nanoclusters synthesized using (a) cavitated template, scale bar = 150 nm; and b) noncavitated template, scale bar = 200 nm.

(17) Wiese, H.; Rupaner, R. *Colloid Polym. Sci.* **1999**, *277*, 372−375.

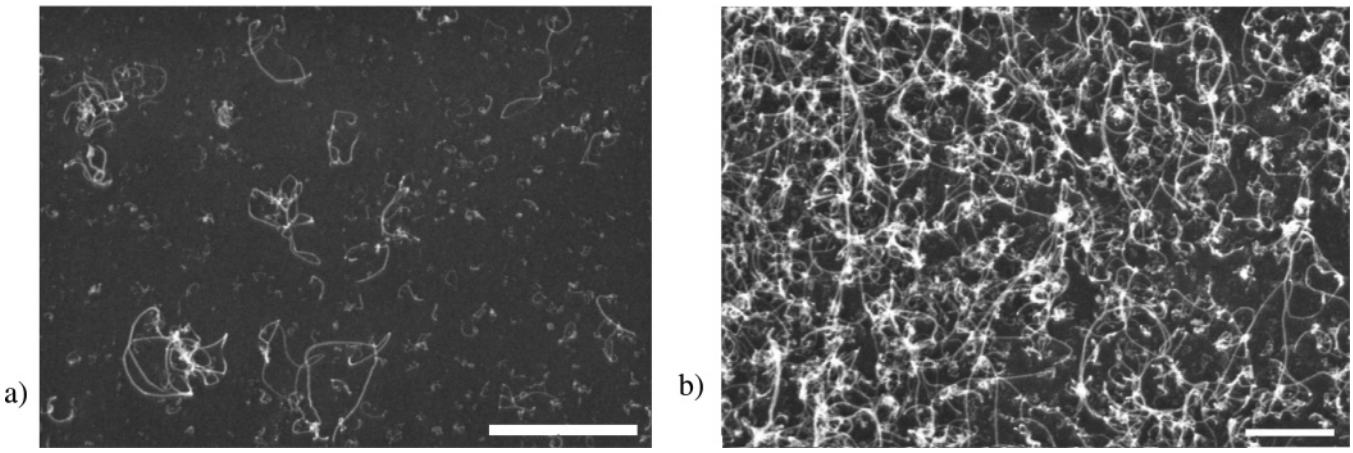

Figure 4. SEM images of 30-min CNT growth on an iron oxide nanocluster array created from a cavitated template: (a) area of low CNT density on substrate, scale bar = 1 um; and (b) area of high CNT density on substrate, scale bar = 500 nm.

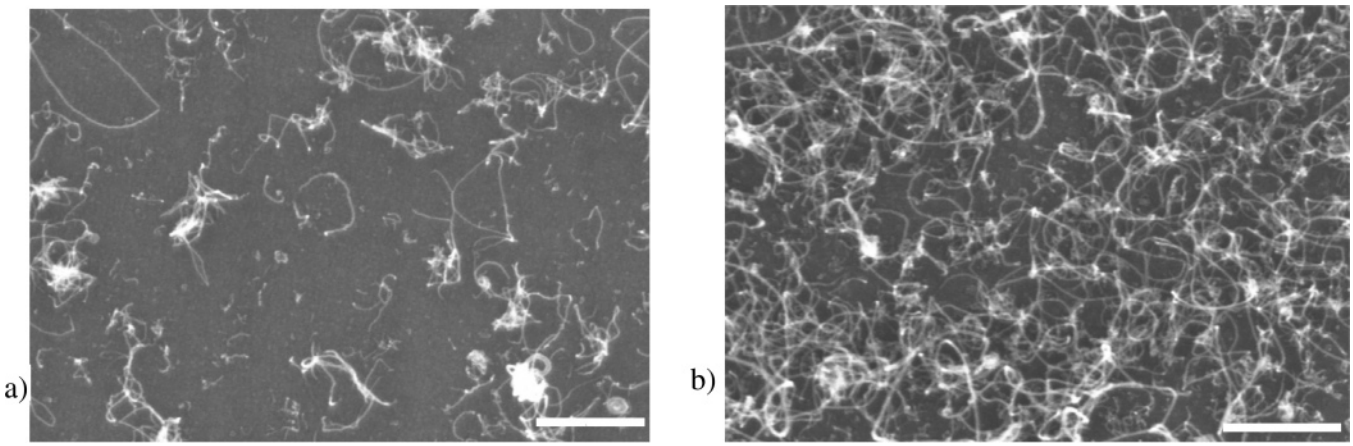

Figure 5. SEM image of 60-min CNT growth on an iron oxide nanocluster array created from a cavitated template: (a) area of low CNT density on substrate, scale bar = 500 nm; and (b) area of high CNT density on substrate, scale bar = 500 nm.

Oxygen plasma etching is an alternative route to thermal degradation to remove the polymer from the substrate surfaces. In the plasma etched samples, the nanoclusters retained their quasi-hexagonal packing over the entire sample surface in all cases. The average diameter of the nanoclusters on the plasma-etched substrates was 10 ± 0.7 nm, the center-to-center spacing was between 29 and 36 nm, and the density was approximately 10^{11} nanoclusters per cm^2.

Carbon Nanotube Growth. We carried out CNT growth experiments to determine the catalytic activity of our iron-containing nanocluster arrays in multiwall CNT (MWCNT) synthesis. Growth times of 10, 30, and 60 min were used. SEM images from the growth process are shown in Figure 4 (30 min growth) and Figure 5 (60 min growth). In many of the samples, the density of CNT varies on the substrate, so both high and low-density regions of CNTs are shown for each sample.

Figure 6 shows TEM images of the iron-containing nanoclusters and the MWCNTs as grown on the substrate surface. Figure 7 shows a high-resolution TEM image of a MWCNT synthesized from iron oxide nanoclusters that were created using the block copolymer micellar thin film template on a silicon wafer. After using high-resolution TEM to image a random sampling of the synthesized MWCNTs, we determined that the MWCNTs have ~8 graphitic layers.

Discussion

Catalytic Substrates. As mentioned in the sample preparation procedure, alterations were made to the original procedure developed by Boontongkong[14] in order to improve the thin film surface coverage and the subsequent surface coverage of the nanocluster arrays. One adjustment involved increasing the concentration of the block copolymer solution from 2.5 mg/mL to 12.5 mg/mL. By increasing the block copolymer concentration, samples with complete surface coverage were created. Other adjustments were reducing the molarity of the NaOH solution and decreasing the time the sample was submerged, thereby creating a thin film that retained near complete surface coverage after cavitation.

As shown in Figure 3b, some areas of the nanocluster arrays produced from noncavitated templates contain iron oxide nanoclusters that lose their quasi-hexagonal order. This occurs during the 20-min 550 °C heating step that is used to degrade the organic material of the cluster-containing block copolymer template. Evidently for the case of noncavitated templates the elevated temperatures allow for increased surface mobility of the iron-containing nanoclusters, but do not lead to significant amounts of coalescence or ripening of the clusters. The surface densities in Figure 3a and b are both equal to $\sim 10^{11}$ particles per cm^2 and the mean diameter is ~7.5 nm in both cases. As mentioned previously, oxygen

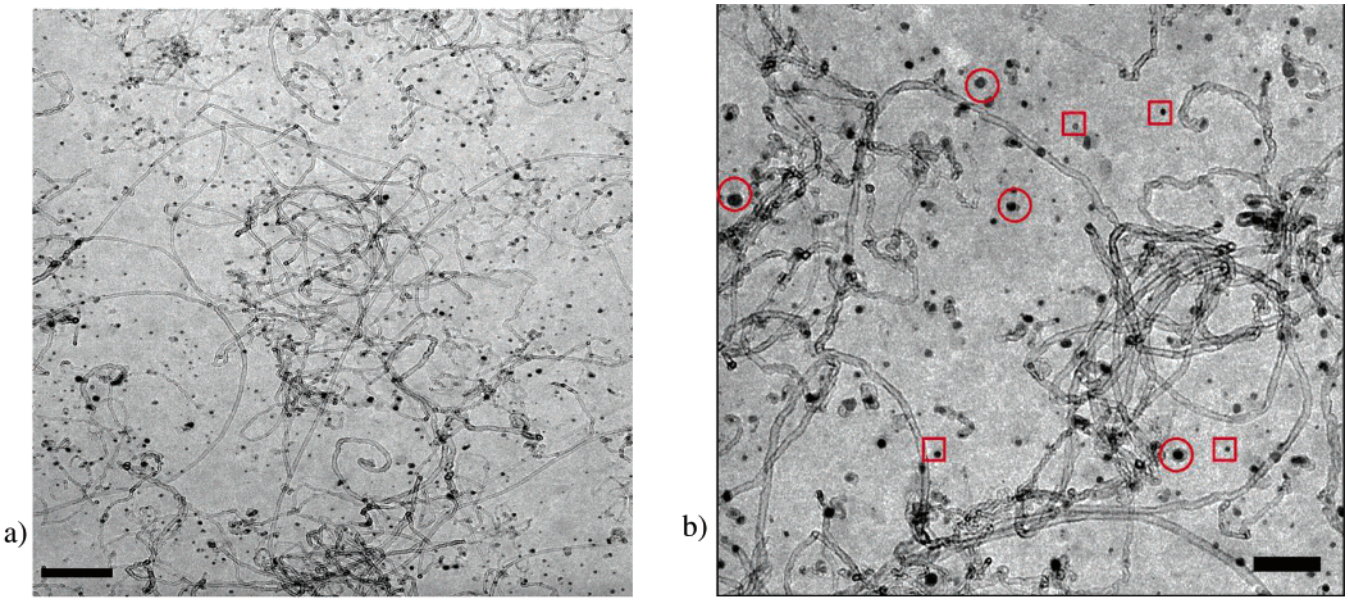

Figure 6. TEM images of 60-min CNT growth on an iron oxide nanocluster array created from a cavitated template. In (a) the scale bar = 200 nm. In (b) circles emphasize examples of nanoclusters with increased diameters after CVD growth (12−14 nm), while squares indicate nanoclusters with diameters similar to the pre-CVD nanocluster diameter (7−9 nm); scale bar = 100 nm.

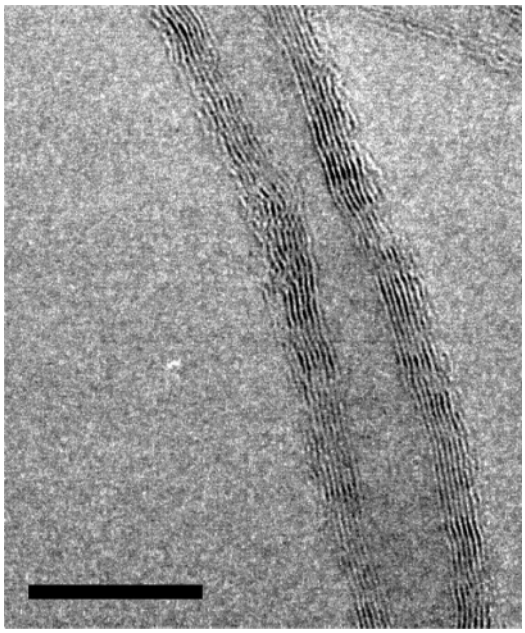

Figure 7. High-resolution TEM image of a multiwall CNT grown from an iron oxide nanocluster on a silicon substrate, scale bar = 10 nm.

plasma etching is an alternative route to remove the polymer without the loss of the nanocluster order on the surface.

Figure 2, a TEM image of a lead-decorated block copolymer template, serves as a reminder of the useful generality[14,15] of the metal cation loading scheme for the case of our PS-*b*-PAA block copolymer templates. The same templates employed in the present Fe-based study can be loaded with Ni, Co, and with any combination of these three magnetic metals. There is no need for synthesizing a new metal-containing block copolymer[13] to study catalytic behavior of these various metals and alloys in CNT growth.

Carbon Nanotube Growth. After characterizing the substrates using both SEM and TEM, it is evident that the proposed block copolymer approach to synthesizing iron-containing nanoclusters, including the use of both cavitated and noncavitated thin films, is a viable route for the production of catalysts for CNT growth. We discovered very similar results in the CNT growths using the nanoclusters created from both the cavitated and noncavitated thin films, so for the remainder of this paper, the discussions will apply to either synthesis route.

To verify that the catalytic activity of the iron oxide nanoclusters is required to enable CNT growth in our experiments, we attempted to grow CNTs on our control substrate, which was identical to all others except for the omission of the iron loading step. By characterizing the sample using both TEM and SEM (images not shown), we found a total absence of CNT growth, demonstrating the need for iron-containing nanoclusters in our CNT synthesis protocol.

The SEM images show that the average length of the CNTs increases as the growth time is increased. From images (not shown) of the substrates subjected to a 10-min CNT growth, the average CNT length was estimated to be ∼100 nm. By examining a substrate after a 60-min CNT growth, shown in Figure 5b, it is clear that the CNTs have an average length that is considerably greater than that achieved in 10 min of growth. In each of the growth times employed, the CNTs exhibit a broad distribution of lengths, which is common for thermal CVD growth processes.[12]

The density of CNTs on the substrate surface also increases with increased CNT growth time. This was qualitatively determined by translating over the substrate surface using SEM. Figure 4a (image of low CNT density from the 30-min growth) is representative of about 40% of the substrate surface. The low-density areas of the 30-min growth samples correspond to approximately 1 CNT per 100 nanoclusters on the substrate surface, while the higher-density areas correspond to approximately 1 CNT per 10 nanoclusters. In contrast to the 30-min growth, Figure 5a (image of

low CNT density from the 60-min growth), represents less than about 25% of the substrate surface. In the 60-min growth, the particles lose their hexagonal arrangement (as demonstrated in the TEM image of Figure 6), and therefore it is exceedingly difficult to estimate the ratio of CNTs to nanoclusters.

On the basis of a variety of SEM images similar to Figures 4 and 5, the average CNT diameter is 11.9 ± 1.5 nm, which is larger than the nanocluster diameter of 7.5 ± 0.8 nm determined from TEM. This is an unexpected result, because previous research[10] has shown that CNTs have diameters slightly smaller than the diameters of the nanoclusters from which they are catalyzed.

Although the SEM images allow for determining trends in the CNT growths, the TEM images of the substrates give a clearer view of the CNT growth and allow for a better quantification of the size of the CNTs relative to the catalytic iron oxide nanoclusters. From the TEM image in Figure 6, the average CNT diameter is 11.8 ± 0.7 nm, which agrees closely with the data from the SEM images. The TEM image also reveals polydispersity in the post-CVD iron-containing nanocluster diameters that was not seen in the originally templated nanocluster precursors. As illustrated in Figure 6b, there is a population of noticeably larger nanoclusters (some are labeled with circles in Figure 6b) with diameters of ~12−14 nm, scattered among the smaller nanoclusters (some are labeled with squares in Figure 6b) with diameters between ~7−9 nm. Examining numerous TEM images like Figure 6 leads to the conclusion that very few of the smaller nanoclusters have successfully catalyzed CNT growth, and most of the CNTs have diameters closely matched to the larger nanocluster diameters. The process by which these larger nanoclusters form is currently unclear, but a possible mechanism might involve the precursor (7.5 nm diameter) nanoclusters initially increasing in size by absorbing carbon atoms to create larger nanoclusters (12−14 nm diameter), followed by carbon precipitation and CNT growth. It is also possible that the smaller nanoclusters fuse to form larger nanoclusters during the high-temperature CNT growth process.

From the TEM images in Figure 6, it is clear that the catalytic iron-containing nanoclusters lose their quasi-hexagonal array over time while exposed to the growth conditions. For the 10-min CNT growth, the TEM image in Figure 8 clearly shows that the iron-containing nanoclusters remain in their quasi-hexagonal arrays. After the growth time is increased to 60 min, the nanocluster quasi-hexagonal arrays appear to be disrupted, as seen in Figure 6. It is unclear at this time whether the disruption of the nanocluster arrays is caused explicitly by the CNT growth process, or if the exposure to high temperature (750 °C) in the CVD growth process plays a central role.

From examining both the SEM and TEM images, we are unable to determine conclusively whether the growth mechanism is tip-growth or base-growth. For a base-growth mechanism to dominate, the iron nanoclusters must interact strongly with the substrate and the nanoclusters must remain on the substrate throughout the growth process. We believe that this growth is catalyzed from the tip of the CNT because the nanoclusters do not appear to be strongly bound to the surface, as demonstrated in Figure 6, where the iron-containing nanoclusters lose their quasi-hexagonal array during the 60-min growth process.

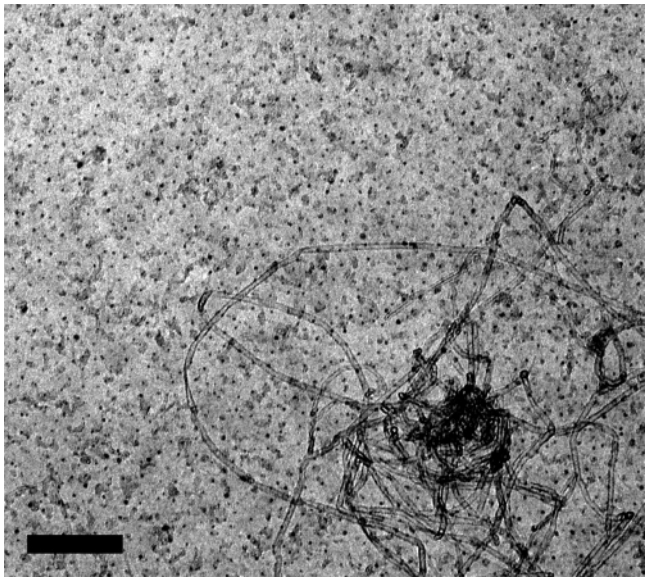

Figure 8. TEM image of a 10-min CNT growth using iron oxide nanoclusters synthesized from a cavitated template on a silicon nitride substrate, scale bar = 100 nm.

In future work, we plan to examine more closely the possible distinctions between the CNTs produced using nanoclusters created from either cavitated or noncavitated thin films. We also plan on using scanning transmission electron microscopy and energy-dispersive X-ray analysis to determine the elements present within the iron-containing nanoclusters after growth, which will help us to better understand the mechanism for the increase in nanocluster diameter. A distinct advantage of this synthesis procedure is the ability to synthesize arrays of different metal-containing nanoclusters from a single block copolymer precursor template. As mentioned above, we plan to utilize this capability to create arrays of other metals known to be catalytically active in CNT growth, such as Ni and Co. We also plan to use these templates to create gold nanocluster arrays for possible applications in the synthesis of zinc oxide nanowires.

Conclusion

In this report, we have demonstrated the ability to create iron-containing nanoclusters with near monodisperse diameters in partially ordered lateral arrays using block copolymer micellar thin films. By varying the spin-casting variables and the concentration of the block copolymer solution, we succeeded in producing a micellar thin film, and subsequently an iron-containing nanocluster array covering more than 90% of the substrate surface. After synthesizing these iron-containing nanoclusters on both silicon nitride and silicon substrates, we used a thermal CVD process to demonstrate their catalytic activity in MWCNT synthesis. By

using silicon nitride membrane window grids as substrates, we were able to characterize, using TEM, the as-grown carbon nanotubes and the catalytic metal nanoclusters while they were still attached to the substrate surface. The block copolymer template offers the possibility of tuning the size and spacing of the metal nanoclusters by altering the block copolymer chain length and composition. It is also straightforward to create nanocluster arrays of different metal species.

Acknowledgment. CMSE Shared Experimental Facilities were used extensively in this work, and the assistance of Mike Frongillo and Libby Shaw is gratefully acknowledged. This work was supported primarily by the Raymond A. and Helen E. St. Laurent Professorship in Chemical Engineering at MIT. The work performed at Boston College is supported by NSF NIRT 0304506.

CM048992L